Analysis Of the Thermal Properties of Sodium Potassium Bismuth Titanate at Morphotropic Phase Boundary Following Photo Pyro Electric (PPE) Method

Nissamuddeen Kunnath
Department of Physics, PSMO College Tirurangadi Malappuram, 676306, India.

***Abstract*—Lead free piezoceramic nanocomposites of Potassium Sodium Bismuth Titanate (KNBT) were synthesized following hydrothermal synthesis and subsequent solid state sintering method. A Morphotropic Phase Boundary (MPB) induced in it through composite preparation with the stochiometric formula (1-x) $K_{0.5}Bi_{0.5}TiO_3$-x $Na_{0.5}Bi_{0.\ 5TiO3.The}$ MPB was confirmed using powder XRD analysis of the composites and microstructure studied using SEM micrographs. The variation of thermal properties of these composites was studied following Photo Pyroelectric Detection (PPE) technique. The analysis of the variation in the thermal properties of these composites give much insight into theory of phonon vibration induced conduction of heat in solids and the way in which various aspects of crystal imperfections controlling it.**

***Index Terms*—Potassium Sodium Bismuth Titanate (KNBT), Morphotropic Phase Boundary (MPB), powder XRD, piezoceramic nanocomposites, Photo Pyroelectric Detection (PPE), phonon vibration.**

I. INTRODUCTION

Studies related to the synthesis and piezoelectric characterization of Bismuth layer structured piezoelectric materials is one of the dynamic areas of research related to development of lead- free piezoelectric materials [1-4]. This category of materials consists of BO_6 octahedral ferroelectric materials like Bismuth Titanate ($Bi_4Ti_3O_{12}$), Lead containing Bismuth layer structured materials with low concentration of lead like Lead Bismuth Niobate ($PbBi_2Nb_2O_9$), and Sodium Bismuth Titanate ($NaBiTiO_3$) that exhibit considerable dielectric permittivity, high Curie temperature and large electro-mechanical coupling coefficients compared to PZT family of piezoceramics [5, 6]. One of the important characteristics of Bismuth based ceramics is that their properties could be enhanced using texturing techniques like hot – forging [7] and hence these grain-oriented ceramics are potential candidate for piezoelectric materials with high Curie temperature, T_C, and they possess anisotropic characteristics which could be used at high temperatures and frequencies. Moreover, this class of materials are found to have large pyroelectric properties as well.

Despite qualities like high Curie temperature, good performance at high frequencies and temperatures and simultaneous exhibition of piezoelectricity and pyroelectricity, Bismuth based materials have low piezoelectric coefficients and dielectric permittivity, resulting in a hindrance to their use as a potential substitute for PZT based ceramics. A widely accepted method to get around this difficulty is to follow new synthesis techniques that offer better controlled texture growth to give the desired grain orientation. Methods like hot – rolling, hot – forging, hot – extrusion etc and topotaxial reactions are the suitable methods to control the grain orientation exploiting dislocations in the grains and making use of the shape of the powder in the raw materials respectively.

The present chapter describes the synthesis and characterization of Bismuth based Potassium Sodium Bismuth Titanate (KNBT) perovskite piezoceramics and their possible applicability as potential piezoelectric materials. The precursor for these KNBT ceramics is Sodium Bismuth Titanate (NBT) which was originally synthesized by Smolenski as early as in 1960 [9], and it was almost at that time PZT was also synthesized and its high piezoelectric response was revealed. NBT is a perovskite- type relaxor ferroelectric with a Curie temperature of 320^0C. It has a rhombohedral structure at room temperature, and shows a relatively large remnant polarization (p_r = 38

$\mu C/cm^2$). However, it is difficult to electrically pole NBT due to a high coercive field (E_c = 7.3 KV/mm) making it difficult to obtain the desirable piezoelectric properties. In addition, unlike PZT ceramics, NBT as such has no MPB occurring in it [10, 11]. Though NBT as such is not piezoelectric, solid solutions like Potassium Sodium Bismuth Titanate (KNBT) possess an MPB structure. Moreover, the KNBT composite can easily be poled and piezoelectricity induced in to it. This material can be produced by forming a binary mixture of Sodium Bismuth Titanate (NBT) and Potassium Bismuth Titanate (KBT) in the desired proportions.

Traditionally KNBT powders are prepared following the solid-state reaction route, with the starting materials being oxides or carbonates of Bi, K, Na or Ti having particle sizes in micrometer or sub micrometer ranges. Generally, this kind of reaction takes place when the components of the mixture having sufficient thermal energy to overcome the atomic/ionic diffusion barriers and hence are possible only at very high perovskite phase forming temperatures. In most cases the resultant powders are not nanocrystalline; they undergo drastic agglomeration and yield inhomogeneous particle sizes as a result of high temperature treatment, making them unfit to enhance further the dielectric or piezoelectric properties for high performance applications.

In contrast to the solid-state reaction route outlined above, hydrothermal synthesis has the potential to produce highly pure and homogeneous metal oxide powders with good control over their stoichiometry, crystallite size and morphology [12, 13]. Recently, utilization of such well-defined metal oxide powders as precursors for piezoelectric ceramics has received much attention, because high performance ceramics close to a MPB have been obtained by texture- treatment [14] or template grain growth [15] utilizing them. As a novel method for preparation of oxide nanopowders, hydrothermal method has the advantage of delivering well-controlled morphology, high purity and narrow particle size distribution for the prepared powders [16].

In this work we report a novel method for the synthesis of solid solutions of Potassium sodium bismuth titanate (KNBT), with stoichiometric formula (1-x) $K_{0.5}Bi_{0.5}TiO_3$-x $Na_{0.5}Bi_{0.5}TiO_3$, by sintering solid solutions of Potassium Bismuth Titanate (KBT) and Sodium Bismuth Titanate (NBT) nanoceramics, synthesized following hydrothermal route at a temperature below 200 ^{0}C, which is much lower than needed for other methods. The prepared KNBT nanopowders have been characterized for their structure by X-ray diffraction and morphology by Scanning electron microscopy. The thermal properties of all these composites were measured using Photo Pyro Electric (PPE) detection method and analysed with the help of phonon vibration theory.

II. EXPERIMENTAL METHODS

2.1. Sample Preparation

For the synthesis of the KNBT composites pure nanopowders of Sodium Bismuth Titanate (NBT) and Potassium Bismuth Titanate (KBT) were separately synthesised following hydrothermal route. For both NBT and KBT analytical grade Bismuth nitrate pentahydrate ($Bi(NO_3)_3.5H_2O$, Alpha Aesar, 98%), Titanium dioxide (TiO_2, Fisher Scientific, 98%) were used as the respective Bismuth and Titanium precursors. The synthesis procedure, as outlined in Chapter 2, was followed in highly alkaline solutions of NaOH and KOH respectively for NBT and KBT respectively. For the synthesis of both NBT and KBT a stoichiometric ratio of 2:1 between Titanium and Bismuth were taken in the starting material.

For the synthesis of pure NBT and KBT nanopowders, Bismuth nitrate was dissolved in CO_2 - free distilled water under vigorous stirring, in to which the corresponding alkali metal hydroxide was added, followed by the addition of Titanium dioxide. After stirring vigorously for about 2 hours, a thin yellow homogeneous solution was formed. The concentrations of Ti^{4+} and Bi^{3+} in the suspension were 0.25 and 0.50 mol/dm^3 respectively, and the alkali metal hydroxide concentration was adjusted to 12 mol/dm^3. The as-prepared mixture was poured in to a Teflon lined autoclave and was then subjected to hydrothermal treatment at 165^{0}C at a comparatively low pressure of 1.5 bars for 72 hours. The so-obtained product was collected and the sediments were washed three times by dispersing in CO_2-free distilled water, followed by centrifuging. The raw powders were then

dried overnight at an ambient temperature of 75^0C. The nanopowders of NBT and KBT obtained in this manner were then calcined at around 650^0C for eight hours. The nanopowders after calcination were analysed for identifying their crystallinity and phase formation using Powder XRD.

Phase pure NBT and KBT nanopowders prepared in this manner were then mixed in different weight ratios and ground well in a mortar, using Polyvinyl alcohol as the binder. KNBT nanocomposites with general formula (1-x) $K_{0.5}Bi_{0.5}TiO_3$ - x $Na_{0.5}Bi_{0.5}TiO_3$, where x = 0, 0.20, 0.25, 0.33, 0.50, 0.75, 0.80, 0.85 and 1.0, synthesized in this manner, were then pelletized to thin discs of 9 mm diameter and 1 mm thickness and then sintered at 50^0C intervals between 850^0C and 1000 ^{0}C for a duration of half-hour each. After heat treatment of the samples, the dry weights of the pellets were measured with a balance and the bulk densities of the sintered samples were determined. The measurement of density is an important step in the processing of ceramic composites since it is a direct indicator of porosity in the material. It is inevitable to obtain composites with extremely minimum porosity percentage as porosity may result in false measurements with high values for dielectric and piezoelectric coefficients. The extent of porosity present in the composites could be identified in terms of their mass density.

2.2. Structural Characterization of the samples

The crystalline phase of the prepared composites in disc form is determined using powder XRD in the θ-2θ mode with Cu-Kα radiation of wave length 1.5406 A^0 (Bruker make, D8 Advance). The lattice parameters (a, b and c) and the unit cell volume (V) were calculated from the obtained XRD data using the MAUD programme. The variation of unit cell parameter with concentration of NBT indicate a change of crystallite phase and is an indication for the possible existence of a Morphotropic phase boundary in the sample.

2.3. Determination of Morphological and Thermal properties

Scanning Electron Microscopy (SEM) with Energy Dispersive X- Ray measurement has been used to identify and characterize the matrix of various compositions. The SEM images of all the samples were recorded with a Scanning electron microscope (Jeol make, Model 6390 LV) to examine the morphology of the matrix and its homogeneity. Energy Dispersive X-ray (EDX) was specifically used to obtain a qualitative information about the full elemental composition of the samples, and to detect any unknown contaminant in the matrix.

The KNBT ceramics were cut and polished for various physical and electrical measurements reported in this work. The thermal properties of KNBT ceramics are measured using the modified photo – pyroelectric (PPE) technique in which the sample, the pyroelectric detector and the backing medium are kept in a thermally thick regime. The sample in thermally thick region is periodically heated via optical absorption of light from an intensity modulated laser beam, which give raise to periodic temperature variations in the sample that ultimately result in thermal wave generation which are detected by a thin (28μm) PVDF film with Ni – Cr coating on both sides being used as a pyroelectric detector. In this experiment, a He – Cd laser having 120 mW power and 442 nm wave length is used as the optical heating source and the intensity modulation is achieved with the help of a mechanical chopper (Stanford Research Systems, Model SR 540). The amplitude and phase of the thermal wave are measured using a dual phase lock-in amplifier (Stanford Research Systems, Model SR 830). The thermal thickness of all the KNBT ceramic composites is verified by plotting the variation of PPE amplitude and phase with modulation frequency at room temperature. Since all the KNBT ceramics used in the measurement are white ceramic pellets with low optical absorption an extremely thin coating of carbon black is provided on the front surface of the sample under illumination, which improves the optical absorption and consequent thermal wave generation, considerably.

In the PPE experimental technique, before conducting the measurement it is necessary to calibrate the experimental set up, and this is accomplished by measuring the thermal properties of the detector by measuring the amplitude and phase of the thermal wave at the detector. Further, during measurements the temperature of the specimen is kept constant to ascertain that the sample gets sufficient time to reach thermal equilibrium.

III. RESULTS

3.1. Structure and Morphology

In the hydrothermal synthesis of metal oxide nanoparticles, the p^H of the super critical reaction medium has a decisive role in the formation rate and crystalline structure of nanoparticles formed [19, 20]. It has been also reported that in the case of perovskite materials like NBT and KBT, initial p^H of the reaction medium influences the crystalline structure and shape of the particles [21, 22]. It has also been reported that a highly alkaline initial p^H of the order of 10 - 12 or at least >10 is necessary for the formation of alkaline Bismuth Titanates as a single phase, and low initial p^H often results in the formation of Bismuth Titanate ($Bi_2Ti_2O_7$) [20] or metallic Bismuth [23]. Figure 1 shows the XRD patterns of hydrothermally treated pure $K_{0.5}Bi_{0.5}TiO_3$, (1-x) $K_{0.5}Bi_{0.5}TiO_3$ - x $Na_{0.5}Bi_{0.5}TiO_3$ (with x = 0. 20, 0.25, 0.33, 0.50, 0.75, 0.80 and 0.85) and pure $Na_{0.5}Bi_{0.5}TiO_3$ nanopowders, all sintered at 1000^0C for three hours. The XRD patterns show well crystallized phases obtained for the samples and the particle sizes estimated using Scherer's formula are found to be around 18 nm, 28 nm, 29 nm, 31 nm, 30 nm, 32nm, 30 nm, 29 nm, and 30 nm respectively for the above samples. The presence of broad diffraction peaks in the case of pure KBT, pure NBT and samples with weight ratio adjusted from 0.25 to 0.75 between KBT and NBT in the solid solution, and with x=0.85 can be assigned as due to the formation of KNBT phase with a rhombohedral crystal structure belonging to R3c space group (JCPDS File No. 01-070-9850) as a major phase [24]. However, in the case of (1-x) $K_{0.5}Bi_{0.5}TiO_3$- x $Na_{0.5}Bi_{0.5}TiO_3$, with x=0.80, the diffraction peaks are sharp, and using JCPDS matching it is found that the diffraction peaks of this structure correspond to a tetragonal phase belonging to the space group P4mm with lattice parameters a = b = 3.761 Å and c = 6.112 Å. The additional peaks corresponding to tetragonal phase are also found to appear for this composition. This clearly indicates a change in phase resulting from a change of concentration, which corresponds to a MPB. The composition range of MPB has also been determined using XRD patterns, which show the coexistence of rhombohedral (R3c) and tetragonal (P4mm) structures in uneven proportion at the composition with x=0.80.

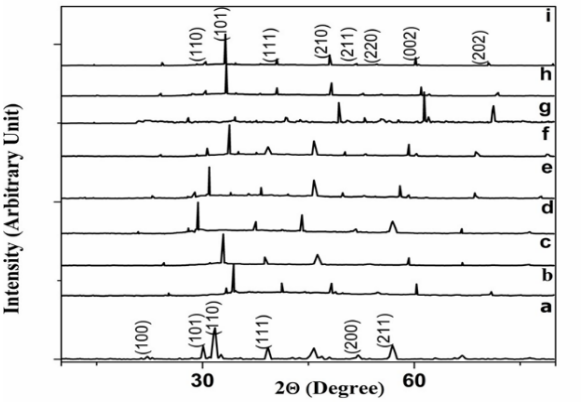

Fig. 1: XRD patterns of hydrothermally synthesized Potassium Sodium Bismuth Titanates, (1-x) $K_{0.5}Bi_{0.5}TiO_3$ - x $Na_{0.5}$ $Bi_{0.5}TiO_3$ with x=0 (pure KBT) (a), 0.20 (b), 0.25 (c), 0.33 (d), 0.50 (e), 0.75 (f), 0.80 (g), 0.85 (h) and 1.00 (pure NBT) (i), all sintered between 850 and 1000^0C for three hours.

The SEM images of all the KNBT ceramics are shown in Figure 2. As is evident from the images the morphology and mean sizes of the resulting particles undergo drastic changes with variation in concentration ratio between KBT and NBT in the composite samples. Nearly spherical fine particles are formed in the case of pure KBT and pure NBT (Figure2 (a, i)), whereas rod-like cubic structures start forming as NBT concentration is increased in the KNBT sample (Figure 2 (d, e, f, g and h)). As can be seen from Figure 2 (g), this rod-like structure formation is at its peak corresponding to the composition (1-x) $K_{0.5}Bi_{0.5}TiO_3$- x $Na_{0.5}Bi_{0.5}TiO_3$, with x = 0.80, whereas such structures start to disappear for the composition (1-x) $K_{0.5}Bi_{0.5}TiO_3$ - x $Na_{0.5}Bi_{0.5}TiO_3$, with x = 0.85 and disappear completely for pure NBT. The average grain sizes of the ceramic particles have been calculated by counting 100 particles visualized from SEM images, and their mean sizes are found to be around 125 nm, 344 nm, 234 nm, 240 nm, 186 nm, 220 nm, 350 nm, 210 nm, and 320 nm respectively for pure KBT, the compositions (1-x) $K_{0.5}Bi_{0.5}TiO_3$ - x $Na_{0.5}Bi_{0.5}TiO_3$, with x = 0.20, 0.25, 0.33, 0.50, 0.75, 0.80, 0.85, and pure NBT. In the case of the composition with x = 0.80 the rod-like structures have an average diameter around 450 nm and length as high as a few micrometers.

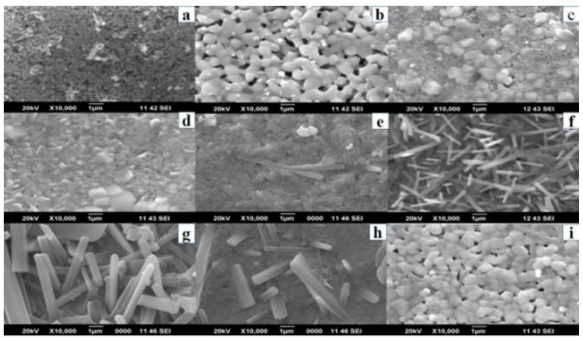

Fig. 2: SEM images of hydrothermally synthesized Potassium Sodium Bismuth Titanates, (1-x) $K_{0.5}Bi_{0.5}TiO_3$ - x $Na_{0.5}Bi_{0.5}TiO_3$ with x=0 (pure KBT) (a), 0.20 (b), 0.25 (c), 0.33 (d), 0.50 (e), 0.75 (f), 0.80 (g), 0.85 (h) and 1.00 (pure NBT) (i), all sintered between 850 and 1000^0C for three hours.

3.2. Sample density and Thermal analysis

The variation of bulk mass density of KNBT samples as a function of NBT concentration is shown in Figure 3. The theoretical density of KBT is 5.929 g/cc and that of NBT is 5.568 g/cc. The theoretical density of various KNBT compositions are calculated as the weighted average of their respective KBT and NBT concentrations. So, as expected, solid solutions of KNBT composites show the corresponding mean values. Moreover, as is evident from Figure 3.3, the measured bulk densities of the samples show good agreement with the corresponding theoretical values and the nature of variations are in good agreement.

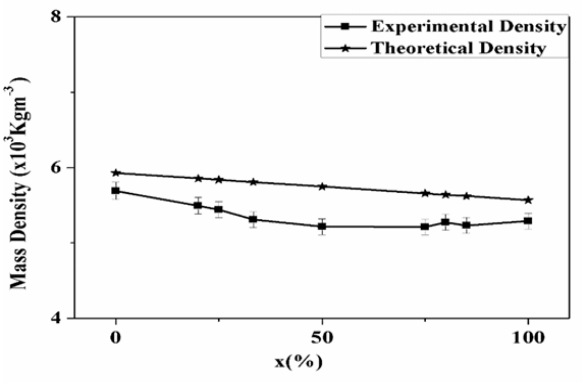

Fig. 3: Variations of theoretical and experimental mass densities with percentage concentration of NBT (x)

Generally, in PPE technique the PPE amplitude will show a raise till the sample reaches thermally thick region, and then falls gradually as the modulation frequency is increased further. However, the PPE phase shows a gradual decrease with modulation frequency. Such variations have been obtained for all the KNBT composites. Variations of the PPE amplitude and phase of a selected representative sample is shown in Figures 4 and 5 respectively. All other samples show similar variations.

The thermal diffusivity and effusivity of the KNBT composites along the direction of the poling axis were determined from the measured PPE amplitude and phase, following the method outlined in Chapter 2. Using the corresponding values of mass density, the thermal conductivity and specific heat capacity for each sample were determined from the values of thermal diffusivity and effusivity using the following equations

$$k = e\sqrt{\alpha} \quad (1)$$

$$C_p = \frac{e}{\rho\sqrt{\alpha}} \quad (2)$$

The variations of various thermal properties of all the KNBT composites with variations in the concentration of NBT have been analysed and are shown in Figure 6. As is evident from the figure the thermal properties increase gradually with increase in concentration of NBT and there is a threshold enhancement in the thermal properties of the composite corresponding to the composition with MPB. Though the presence of MPB has nothing to do with the thermal properties, the frequency of phonons in the solid has some crucial role on the thermal properties of the solid and is a parameter that strongly depend on phonon mean free path and the presence of lattice distortions and defects [33].

Fig. 4: Frequency dependence of photopyroelectric amplitudes with modulation frequency at room temperature for the samples shown in the inset.

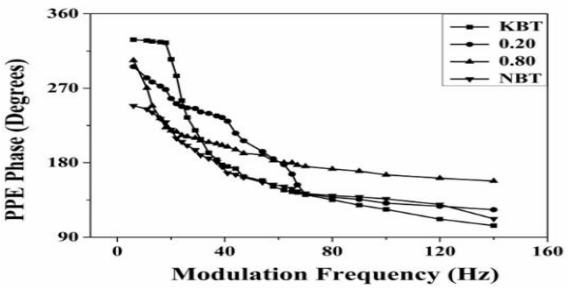

Fig. 5: Frequency dependence of photopyroelectric phases with modulation frequency at room temperature for the samples shown in the inset.

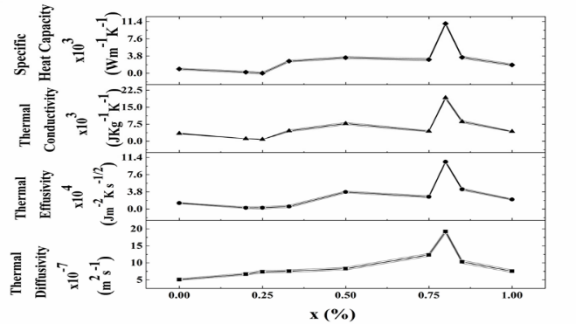

Fig. 6: Variations of thermal diffusivity, thermal effusivity, thermal conductivity and specific heat capacity for KNBT samples with percentage composition of NBT (x)

IV. DISCUSSION OF RESULTS

Measurement of the density of various composites shows that the extent of porosity in various compositions is extremely small and the sintering is very good so that porosity induced property change is not exhibited by the samples.

In order to confirm the MPB of KNBT ceramics observed at the composition with x = 0.8, an evaluation of the lattice parameters and the unit cell volume with concentration of NBT have been done using MAUD programme for all the compositions and are tabulated in Table 1. The unit cell volume initially shows an increase and then falls slightly for the composition with x=0.5 and then remains almost constant. This is reflected in the XRD pattern also (Figure 1) as a shift in the peak position for the corresponding compositions. Compared to pure NBT and KBT the lattice parameters a, b and c more or less remain equal and constant for composition with $x \leq 0.5$. However, for the composition with $x > 0.5$, a and b fall slightly whereas c increases considerably. This increase is at its peak for the composition with x=0.8 at a value of 6.112 A^0. This indicates that due to the coexistence of NBT and KBT in different weight ratios, the structure starts changing from rhombohedral to tetragonal from x=0.5 onwards and is distinctly in tetragonal phase for the composition with x=0.8.

Table 1: Lattice parameters of KNBT ceramics

Lattice Parametersx						
x	*a* (A^0)	*b* (A^0)	*c* (A^0)	*V* ($A^{0\,3}$)	*b/a*	*c/a*
0.00	3.973±.001	3.989±.001	3.989±.001	63.206	1.004	1.004
0.20	4.241±.001	4.241±.001	4.241±.001	76.268	1.000	1.000
0.25	4.243±.001	4.245±.001	4.247±.001	76.502	1.001	1.001
0.33	4.119±.001	4.123±.001	4.587±.001	77.903	1.001	1.113
0.50	4.197±.001	4.199±.001	4.957±.001	87.342	1.000	1.181
0.75	4.022±.001	4.026±.001	5.548±.001	89.823	1.001	1.380
0.80	3.761±.001	3.761±.001	6.112±.001	86.936	1.000	1.625
0.85	3.988±.001	3.989±.001	5.524±.001	87.85	1.000	1.385
1.00	4.236±.001	4.238±.001	4.328±.001	77.696	1.000	1.022

The tetragonal distortion in the samples has also been evaluated, and are also shown in Table 1. It is found that the rhombohedral distortion (b/a) almost remains constant at unity for all compositions whereas tetragonal strain constant (c/a), though remains almost unity for x<=0.5, start increasing up to a maximum of almost 63% at composition with x=0.8. This further indicates that a change of composition results in a change of phase from rhombohedral to tetragonal resulting in an MPB at the composition with x=0.8. It can further be noticed from the Table that the MPB is stable for a range of concentration $\Delta x = 0.05$ on either side of x = 0.8. After this range the tetragonal strain constant falls to around 38% from around 63% at the MPB. It may also be noted here that the unit cell volume though constant for compositions with x>0.5 it shows a slight increase for composition with x=0.75. This hss resulted from the simultaneous fall of the lattice parameters a and b along with an elongation for the lattice parameter c, as this composition is

reached. However, the tetragonal strain constant (c/a) still increases to show a maximum value at x=0.8. This is shown in Figure 7. It is evident from the figure that corresponding to the composition for which x = 0.80 the tetragonal strain constant increases; at the same time the rhombohedral distortion b/a falls correspondingly. This results in a drastic distortion for the lattice for the composition corresponding to x = 0.80.

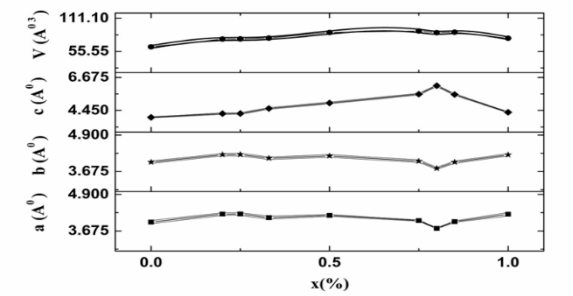

Figure 7: Variation of lattice parameters with percentage concentration of NBT (x) for KNBT ceramic composites.

The above argument is further confirmed in microstructure analysis by SEM. Among the various KNBT ceramics the grain size is found to be minimum in the case of pure KBT and it is found to increase as the concentration of NBT is increased. It appears that higher concentration of KBT in the composite sample generally inhibits grain growth; however, a considerable population of NBT in the sample enhances grain growth as can be seen in Figures 2 (d-h). In such NBT dominant ceramics the domains of most of the grains are lamellar or needle-shaped and is an indicator for the formation of tetragonal domains, and this result is in agreement with the studies reported earlier by Octonicar et al [25]. A more detailed discussion on the actual mechanism of domain formation close to MPB requires neutron scattering or selected area electron diffraction studies of the compositions.

Further, the above modification results in lattice distortion which is supposed to lead to enhanced polarizability [31, 32]. It is anticipated to be beneficial to enhancement in dielectric and piezoelectric properties of the material.

The variations of thermal diffusivity (α), effusivity (e), thermal conductivity (k) and specific heat capacity (C_p) with concentration of NBT, as shown in Figures 4,5 and 6, clearly indicate that the above thermal properties undergo an anomalous behaviour as the phase transformation takes place. Figure 3.6 clearly shows that the thermal parameters exhibit maxima at the composition with MPB. Further, there is an overall enhancement in the thermal conductivity in the KNBT composite with MPB. This anomalous raise in the thermal conductivity at the MPB can be explained in terms of the increase in mean free path of phonons resulting from a corresponding fall in the phonon - phonon and phonon – defect collision rates. The anomalous behaviour in the specific heat capacity may be attributed to softening of phonon modes and the consequent reinforcing contribution of phonon modes to the specific heat capacity.

The general expression for the thermal conductivity of a solid is given by,

$K = \frac{1}{3} C_v l$ (3)

were,

C = phonon specific heat,

v = phonon group velocity, and

l= phonon mean free path.

A lattice distortion can affect the phonon mean free path via scattering [34] and hence can cause anomalous behaviour in the composition corresponding to MPB and also in those close to MPB. The enhancement in thermal conductivity could be viewed as a raise in the same over the expected thermal conductivity in the absence of lattice distortion. Let K_{bg} be the expected 'back ground' thermal conductivity in the absence of the lattice distortion and K the actual observed thermal conductivity, then the enhancement in thermal conductivity is $K - K_{bg}$. Levanyuk et al have noticed that in ferroelectric crystals the order parameter ρ affect the thermal conductivity (k) through the equation [35, 36]

$K = K_{bg} + \frac{c_0^2 T \rho^2}{\gamma}$ (4)

Were,

C_0 and γ are constants, T is the temperature and ρ is the magnitude of the order parameter.

From the preceding analysis we see that in the KNBT composite with x =0.80, there occurs the coexistence of tetragonal and rhombohedral phases which provide a large number of ferroelectric domain orientations. Accommodation of tetragonal and rhombohedral phases make the composition highly viable to crystal distortion thereby leading to extraordinary behavior towards thermal properties.

V. CONCLUSIONS

Nano particles of Sodium Bismuth Titanate (NBT) and Potassium Bismuth Titanate were synthesised following hydrothermal method. Various nanocomposites Potassium Sodium Bismuth Titanate with particle size bellow 100 nm were obtained by making solid solutions of pure NBT and KBT in different weight ratios, followed by high temperature sintering. The method offers a novel and simple route for the synthesis of high-quality ceramics in powder form with particle dimensions in nanometer scales. Analysis shows that the composition around $K_{0.2}Na_{0.8}BiTiO_3$ undergoes a microstructural phase change from rhombohedral to tetragonal structure, which is identified as a Morphotropic phase boundary. The piezoelectric properties show threshold maxima at this composition, and are comparable to the well-known PZT. The thermal properties of all the KNBT samples are also reported, which show threshold behavior at the phase boundary. The results reveal the potential of the procedure followed in this work for the development of lead-free piezoelectric nanoceramics to replace PZT for the development of sensors and actuators.

REFERENCES

[1] Armstrong, R. A., and R. E. Newnham. "Bismuth titanate solid solutions." Materials Research Bulletin 7.10 (1972): 1025-1034.

[2] Aoyagi, Rintaro, et al. "Piezoelectric properties of vanadium- substituted strontium bismuth niobate." Japanese Journal of Applied Physics 44.9S (2005): 7055.

[3] Ando, Akira, Masahiko Kimura, and Yukio Sakabe. "Piezoelectric properties of Ba and Ca doped $SrBi_2Nb_2O_9$ based ceramic materials." Japanese Journal of Applied Physics 42.2R (2003): 520.

[4] Ando, Akira, Masahiko Kimura, and Yukio Sakabe. "Piezoelectric resonance characteristics of $SrBi_2Nb_2O_9$-based ceramics." Japanese Journal of Applied Physics 42.1R (2003): 150.

[5] Takenaka, Tadashi. "Bismuth-based piezoelectric ceramics." Piezoelectric and Acoustic Materials for Transducer Applications. Springer, Boston, MA, 2008. 103-130.

[6] Ikegami, Seiji, and Ichiro Ueda. "Piezoelectricity in ceramics of ferroelectric bismuth compound with layer structure." Japanese Journal of Applied Physics 13.10 (1974): 1572.

[7] Takenaka, Tadashi, Kyo Komura, and Koichiro Sakata. "Possibility of new mixed bismuth layer-structured ferroelectrics." Japanese Journal of Applied Physics 35.9S (1996): 5080.

[8] Takenaka, Tadashi, and Hajime Nagata. "Current status and prospects of lead-free piezoelectric ceramics." Journal of the European Ceramic Society 25.12 (2005): 2693-2700.

[9] G. A. Smolenskii, V. A. Isupov, A. I. Agranovskaya and N. Krainik, “New Ferroelectrics of Complex Composition” Sov Phys. Solid State 2 2651- 54 (1961)

[10] Sasaki, Atsushi, et al. "Dielectric and piezoelectric properties of $(Bi_{0.5}Na_{0.5})TiO_3$–$(Bi_{0.5}K_{0.5})TiO_3$ systems." Japanese Journal of Applied Physics 38.9S (1999): 5564.

[11] Rödel, Jürgen, et al. "Perspective on the development of lead-free piezoceramics." Journal of the American Ceramic Society 92.6 (2009): 1153-1177.

[12] Li, Yueming, et al. "Dielectric and ferroelectric properties of lead- free Na0. 5Bi0. 5TiO3–K0. 5Bi0. 5TiO3 ferroelectric ceramics." Ceramics International 31.1 (2005): 139-142.

[13] Sugimoto, Tadao. Monodispersed Particles. Elsevier, 2019.

[14] Waseda, Yoshio, and Atsushi Muramatsu, eds. Morphology control of materials and nanoparticles: Advanced materials processing and characterization. Vol. 64. Springer Science & Business Media, 2003.

[15] Horn, Jeffrey A., et al. "Templated grain growth of textured bismuth titanate." Journal of the American Ceramic Society 82.4 (1999): 921-926.

[16] Villafuerte-Castrejón, María Elena, et al. "Towards lead-free piezoceramics: Facing a synthesis challenge." Materials 9.1 (2016): 21.

[17] Nye, John Frederick. Physical properties of crystals: Their representation by tensors and

matrices. Oxford university press, 1985.

[18] Jaffe, Bernard. Piezoelectric Ceramics. Vol. 3. Elsevier, 2012.

[19] Rödel, Jürgen, et al. "Perspective on the development of lead-free piezoceramics." Journal of the American Ceramic Society 92.6 (2009): 1153-1177.

[20] Tani, Toshihiko. "Crystalline-oriented piezoelectric bulk ceramics with a perovskite-type structure." Journal of the Korean Physical Society 32.9 (1998): 1217.

[21] Horn, Jeffrey A., et al. "Templated grain growth of textured bismuth titanate." Journal of the American Ceramic Society 82.4 (1999): 921-926.

[22] Lencka, Malgorzata M., Magdalena Oledzka, and Richard E. Riman. "Hydrothermal synthesis of sodium and potassium bismuth titanates." Chemistry of Materials 12.5 (2000): 1323-1330.

[23] Kanie, Kiyoshi, et al. "Synthesis of bismuth sodium titanate fine particles with different shapes by the gel-sol method." Materials Transactions 48.8 (2007): 2174-2178.

[24] Moulson, Anthony J., and John M. Herbert. Electroceramics: materials, properties, applications. John Wiley & Sons, 2003.

[25] Otonicar, Mojca, Sreco D. Skapin, and Bostjan Jancar. "Tem analyses of the local crystal and domain structures in (na 1-x k x) 0.5 bi 0.5 tio 3 perovskite ceramics." IEEE transactions on ultrasonics, ferroelectrics, and frequency control 58.9 (2011): 1928-1938.

[26] Wang, Chun-Ming, and Jin-Feng Wang. "Aurivillius phase potassium bismuth titanate: K0. 5Bi4. 5Ti4O15." Journal of the American Ceramic Society 91.3 (2008): 918-923.

[27] Hooker, Matthew W. "Properties of PZT-based piezoelectric ceramics between 150 and 250 C." (1998).

[28] Krueger, H. H. A., and Don Berlincourt. "Effects of high static stress on the piezoelectric properties of transducer materials." The Journal of the Acoustical Society of America 33.10 (1961): 1339- 1344.

[29] Zhang, X. L., et al. "Dielectric and piezoelectric properties of modified lead titanate zirconate ceramics from 4.2 to 300 K." Journal of Materials Science 18.4 (1983): 968-972.

[30] Karapuzha, A. S., et al. "Structure, dielectric and piezoelectric properties of donor doped PZT ceramics across the phase diagram." Ferroelectrics 504.1 (2016): 160-171.

[31] Miyayama, Masaru, and Yuji Noguchi. "Polarization properties and oxygen-vacancy distribution of SrBi2Ta2O9 ceramics modified by Ce and Pr." Journal of the European Ceramic Society 25.12 (2005): 2477-2482.

[32] Jiang, Xiang-Ping, et al. "High performance Aurivillius type $Na_{0.5}Bi_{4.5}Ti_4O_{15}$ piezoelectric ceramics with neodymium and cerium modification." Journal of Advanced Ceramics 4.1 (2015): 54-60.

[33] Philip, J., and M. V. Manjusha. "Thermal transport across incommensurate phases in potassium selenate: photo- pyroelectric and calorimetric measurements." Journal of Physics: Condensed Matter 21.4 (2008): 045901.

[34] Ortiz, Brenden R., et al. "Effect of extended strain fields on point defect phonon scattering in thermoelectric materials." Physical Chemistry Chemical Physics 17.29 (2015): 19410-19423.

[35] Levanyuk, A. P., S. A. Minyukov, and M. Vallade. "Elastic anomalies at structural phase transitions: a consistent perturbation theory. I. One component order parameter." Journal de Physique I 2.10 (1992): 1949-1963.

[36] Lebedev, N. I., et al. "Elastic anomalies at structural phase transitions: a consistent perturbation theory. II. Two-component order parameter including the case of incommensurate phase." Journal de Physique I 2.12 (1992): 2293-2297.

[37] Isupov, V. A. "The range of coexistence of phases in lead zirconate–titanate solid solutions." Sov. Phys. Solid State 10 (1968): 989.